

Facile and Sustainable Modification for Improving the Adsorption Ability of Sugarcane Bagasse Towards Cationic Organic Pollutants

Pengcheng Luan

South China University of Technology <https://orcid.org/0000-0001-8896-3263>

Jianming Liao

South China University of Technology

Li Chen

South China University of Technology

Yishan Kuang

South China University of Technology

Xi Zhang

South China University of Technology

Yuxiang Zhang

South China University of Technology

Yikui Zhu

South China University of Technology

Yonghong Dai

Guangxi Boguan Environmental Products Co., Ltd.

Lihuan Mo

South China University of Technology

Jun Li (✉ ppjunli@scut.edu.cn)

South China University of Technology <https://orcid.org/0000-0001-8242-6184>

Research Article

Keywords: sugarcane bagasse, ozone modification, cationic organic pollution, biosorption

Posted Date: November 16th, 2021

DOI: <https://doi.org/10.21203/rs.3.rs-1029529/v1>

License:   This work is licensed under a Creative Commons Attribution 4.0 International License.

[Read Full License](#)

Version of Record: A version of this preprint was published at Biomass Conversion and Biorefinery on March 24th, 2022. See the published version at <https://doi.org/10.1007/s13399-022-02551-9>.

1 **Facile and sustainable modification for improving the adsorption** 2 **ability of sugarcane bagasse towards cationic organic pollutants**

3 Pengcheng Luan[#], Jianming Liao[#], Li Chen, Yishan Kuang, Xi Zhang, Yuxiang Zhang, Yikui
4 Zhu, Yonghong Dai, Lihuan Mo, Jun Li*

5 **Abstract:** Using low-cost agro-industrial wastes and by-products derived from
6 lignocellulosic biomass for adsorption is believed to an affordable and sustainable way to tackle
7 the burning issue of cationic pollution in the marine, while its relatively low adsorption
8 capability limits its large-scale application. Chemical modifications to improve the adsorption
9 abilities of lignocellulosic biomass usually has problems such as long reaction time, high
10 operational cost, rigorous reaction conditions (high temperature and pressure) as well as the
11 second pollution. In this study, a green, rapid, simple, and mild method was developed by using
12 ozone to improve the adsorption abilities of sugarcane bagasse (SB). The effects of ozone

Jun Li* - *State Key Laboratory of Pulp and Paper Engineering, South China University of Technology, Guangzhou, 510641, China; Email: ppjunli@scut.edu.cn*

Pengcheng Luan[#] - *State Key Laboratory of Pulp and Paper Engineering, South China University of Technology, Guangzhou, 510641, China*

Jianming Liao[#] - *State Key Laboratory of Pulp and Paper Engineering, South China University of Technology, Guangzhou, 510641, China*

Li Chen - *State Key Laboratory of Pulp and Paper Engineering, South China University of Technology, Guangzhou, 510641, China*

Yuxiang Zhang - *State Key Laboratory of Pulp and Paper Engineering, South China University of Technology, Guangzhou, 510641, China*

Yikui Zhu - *State Key Laboratory of Pulp and Paper Engineering, South China University of Technology, Guangzhou, 510641, China*

Yonghong Dai - *Guangxi Boguan Environmental Products Co., Ltd., Guangxi, 547000, China*

Lihuan Mo - *State Key Laboratory of Pulp and Paper Engineering, South China University of Technology, Guangzhou, 510641, China*

[#] P. L. and J.L. contributed equally to this work.

13 modification on the SB and its related adsorption abilities towards cationic polymers were
14 quantitatively investigated. Results showed that ozone modification under very low ozone
15 consumption (~ 1.5 wt%) could efficiently increase the carboxyl groups, change the chemical
16 compositions of SB, and does not significantly change its morphology, thereby ensuring the
17 good recovery and adsorption performance of SB. The maximum adsorption rate and capacity
18 of SB for positively charged methylene blue (MB) were increased about 33.3% and 11.3% than
19 the original SB. Besides, ozone modified SB maintained its high adsorption capability even at
20 high NaCl concentration (0.6 M). For cationic polymer with high charge densities, the
21 adsorption capacity of milled SB increased about 125.4%.

22 **Key words:** sugarcane bagasse, ozone modification, cationic organic pollution, biosorption

23 **Introduction**

24 Ocean, accounting for 71% of the total area of the earth, is of crucial importance not only
25 to the worldwide energy systems but also to the nutrient supplies. Statistics show that more
26 than 155 million tons of seafood are taken from the ocean every year, providing at least 20%
27 of total animal proteins for 3.1 billion people.¹ Besides, they are also important sources of
28 amino acids, micronutrients, vitamins, and the only natural dietary source of n-3
29 polyunsaturated fatty acids, which are essential for the normal growth of young children.²
30 However, with the fast development of world industry in recent decades and occasionally
31 occurred marine pollution emergencies, marine pollution has seriously damaged the marine
32 ecological environment and thus adversely affected the food safety of seafood. Major marine
33 pollutants include chemicals and plastics. Among them, cationic organic pollutants, such as

34 cationic dyes (MB, methyl orange, etc.), are one of the main chemical pollutants, which have
35 strong carcinogenic and mutagenic effects and can enter into the human consumers' bodies by
36 the bioaccumulation, causing long-term toxic effects.³ Moreover, in the marine environment,
37 cationic organic pollutants have the features of long duration, wide spreading, and difficult to
38 control. Therefore, effective removal of cationic organic pollutants in the ocean is urgent and
39 necessary.

40 Currently, the main strategies for the removal of cationic organic pollutants in the water
41 bodies include physical (adsorption, membrane separation, etc.), chemical (oxidation,
42 coagulation, etc.), and biological methods (aerobic and anaerobic treatment) or a combination
43 of two or three above methods.⁴ However, since most cationic organic pollutants have high
44 resistance due to their complex chemical structure and the particularity of the marine
45 environment (high salinity and vast area), most of the above methods are costly, poorly feasible,
46 and have secondary pollution concerns.

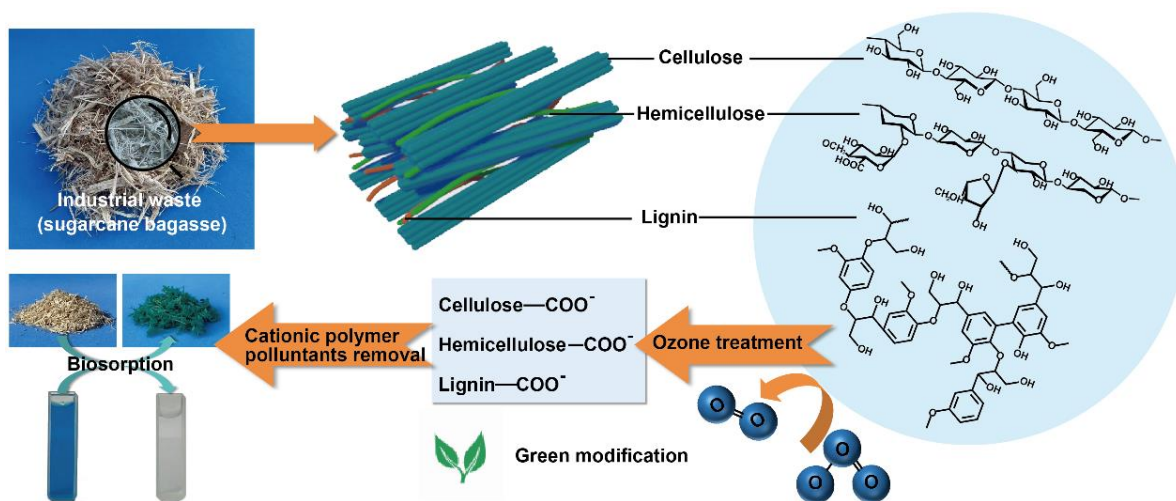
47 Recently, adsorption by using low-cost lignocellulosic biomass, especially for the agro-
48 industrial wastes and by-products, to remove the cationic organic pollutants from the marine
49 environment is considered a promising technology because of its simple operation process and
50 high feasibility.⁵ Among those agro-industrial wastes and by-products, sugarcane bagasse (SB),
51 in the form of pulpy fibrous material, is the main by-product of sugar industry after crushing
52 the sugarcane to extract their juice. Because sugarcane from Nature is the world's largest crop
53 by production quantity with an annual output of more than 1.8 billion tons, SB is a widely
54 available, cost effective, sustainable, and carbon neutral material. SB is commonly used as the
55 primary fuel source for sugar mills and sometimes for pulping. The use of low-cost SB to

56 adsorb cationic pollutants can realize the reuse of resources and is sustainable and affordable.
57 Moreover, the SB after adsorption can be regenerated for continued use or burned to provide
58 energy. Nevertheless, for large-scale applications, the main limitation of SB is their relatively
59 low adsorption capacity due to their very limited anionic groups.⁵ Furthermore, the complexity
60 of SB, mainly composed of cellulose (45-55 wt%), hemicellulose (20-25wt%), and lignin (18-
61 24 wt%) (Figure 1),⁶ makes it difficult to be efficient chemical modified towards all three
62 components. Various agents have been used to cationic modify the lignocellulosic biomass,
63 including acids (citric acid, succinic anhydride, acrylonitrile, and 2-mercaptobutanedioic acid),
64 bases (sodium hydroxide and sodium carbonate), oxidants (periodate, sodium hypochlorite,
65 and potassium permanganate), and many other chemical compounds (thionyl chloride,
66 epichlorohydrin, acrylonitrile, and hydroxylamine).^{7, 8} However, most of those modification
67 reactions need long reaction time, high operational cost, and rigorous reaction conditions (high
68 temperature and pressure). Additionally, extra efforts need to be paid to the second pollution
69 caused by the modification reactions. Therefore, finding green modification ways to improve
70 the adsorption performance of lignocellulosic biomass has a practical significance.

71 Ozone represents a promising modification reagent for increasing the anionic groups of
72 materials because it's reactive, green, and cheap. Ozone is a strong oxidant with an extremely
73 high oxidation potential of 2.07 eV. It has been used to react with oxidizable organics and even
74 inorganic substances under normal temperature and pressure into products with carbonyl or
75 carboxyl groups. For lignocellulosic biomass, previous studies showed that ozone could
76 oxidize all three main components of lignocellulosic biomass (cellulose, hemicellulose, and
77 lignin) into carboxyl-containing structures, indicating the feasibility of using ozone

78 modification to increase its adsorption performance. Additionally, both the raw material and
79 reaction product of ozone are usually oxygen, indicating the green nature of ozone modification.

80 In this study, we developed a simple and green method by using ozone to increase the
81 adsorption performance of sugarcane bagasse (SB) under normal temperature and pressure
82 (Figure 1). The effects of ozone on the chemical compositions, total and surface anionic groups
83 (carboxyl groups), and the absorption behavior of SB were investigated. Two types of cationic
84 polymers were chosen in this study to verify the adsorption abilities of the ozone modified SB
85 towards cationic pollutants with different charge densities, including poly dimethyl diallyl
86 ammonium chloride (PDADMAC) with a high charge density and MB with a low charge
87 density. Ozone modified SB showed enhanced adsorption capability towards cationic organic
88 pollutants in the aqueous environment with low ozone consumption and high yield.
89 Considering ozone as an efficient and green reactant, ozone modified lignocellulosic biomass
90 could be a promising adsorbent for removal of the cationic organic pollutants in the marine.



91
92 **Figure 1.** Ozone modification of industrial waste (sugarcane bagasse) to increase its anionic
93 groups for cationic organic pollutants.

94 **Materials and methods**

95 **Materials.** SB grown in South China was provided by a local pulp mill (Guangxi). It was
96 washed three times with distilled water and dried at 60°C before use. The dried SB was ground
97 and crushed into small pieces by using a cutting mill (CM 200, Beijing Grinder Instrument Co.,
98 Ltd., China) equipped with a 4-mesh discharge screen. The crushed SB powder was vibrating
99 separated by a circular vibrating screen (8411, Shangyu fifty-four Instrument Factory, China).
100 The 20-40 mesh fraction of SB was collected and used in this experiment. Analytical grade
101 H₂SO₄, NaOH, NaCl, and MB were used in this study.

102 **Ozone treatment.** 10 g of SB was firstly treated by 10 wt% H₂SO₄ at pH 2.0 for 30 min.
103 Then the mixture was diluted by H₂SO₄ solution (pH = 2.0) to 40 wt% consistency. The
104 obtained SB was transferred to a gas washing bottle. Ozone was fed from the bottom of stacked
105 bagasse for 2.5 min, 5.0 min, 7.5 min, and 10.0 min, respectively. Ozone generator (GM 3,
106 Primozone, Sweden) was used to generate ozone. The ozone concentration was detected by an
107 ozone concentration detector (UV-2100, Usideal, China). The whole process was conducted
108 under normal temperature (23-25°C) and pressure. Ozone consumption under different
109 treatment time was listed in Table 4.

110 **Table 4.** Ozone consumption at different treatment time.

Sample	Ozone concentration (g/m ³)	Flow rate (L/min)	Time (min)	Ozone consumption (%)
0	0.0	0.0	0.0	0.0
1	154.7	1.5	2.5	1.5
2	156.5	1.5	5.0	3.0
3	152.2	1.5	7.5	4.4
4	166.8	1.5	10.0	7.7

111

112 **Morphology of SB.** Field emission scanning electron microscopy (FE-SEM, Merlin
113 Compact, Zeiss, Germany) was used to investigate the morphology of SB at the ozone dosage
114 of 0, 1.5 wt%, and 7.7 wt%.

115 **FTIR analysis of SB.** Pellets of FTIR samples were prepared by mixing with 200 mg of
116 spectroscopic grade KBr and 1 mg milled SB. IR spectra (4000–400 cm⁻¹) were recorded using
117 a Nicolet 520P spectrometer with a resolution of 4 cm⁻¹ and 64 scans per sample.

118 **Composition analysis of SB.** The contents of cellulose, hemicellulose, and lignin in SB
119 were examined according to NREL/TP-510-42623 issued by National Renewable Energy
120 Laboratory (NREL). 0.3 g benzene-alcohol extracted SB was treated by a double -stage H₂SO₄
121 hydrolysis (1st stage: 72% acid, 30° C, 1h; 2nd stage: 4% acid, 121 ° C, 1h). The obtained
122 hydrolysate was then filtered by G₄ filter with constant weight. The hydrolyzed
123 monosaccharides were performed using High Performance Liquid Chromatography (HPLC,
124 Agilent 1260, Agilent Technologies, USA). The acid-soluble lignin was performed using
125 Visible UV Spectrophotometer (UV2600, Shimane Shimadzu Corporation, Japan). The G₄
126 filter was washed by distilled water until the filtrate was neutral and transferred into oven at
127 105 ° C to a constant weight. Then transfer the filter to a muffle furnace for calcination at 575
128 ±25° C for 4h to obtain the weight of its ash. The weight of the solid residue after deducting
129 the weight of its ash is the weight of acid-insoluble lignin.

130 The selectivity coefficient of ozone towards lignin and carbohydrates (cellulose and
131 hemicellulose) is calculated as follows:

$$\text{Selectivity}_{n-(n+1)} = \frac{\text{Lignin}_n - \text{Lignin}_{n+1}}{\text{Carbohydr}_n - \text{Carbohydr}_{n+1}} \quad (1)$$

132 Where Selectivity_{n-(n+1)} represents the selectivity coefficient of ozone at the phase of n-
133 (n+1); Lignin_n and Carbohydr_n represent the lignin content (mg) and carbohydrates (mg) of
134 Sample n, respectively; Lignin_{n+1} and Carbohydr_{n+1} represent the lignin content (mg) and
135 carbohydrates (mg) of Sample_{n+1}, respectively.

136 **Determination of the total carboxyl and carbonyl groups in SB.** Before the determination,
137 the ozone-treated SB was milled into powder by the planetary ball mill (PQ-N2, Across
138 International, USA). The total carboxyl content in SB was determined by conductometric
139 titration. About 0.3 g of milled SB and 5 mL of 0.01 mol/L NaCl solution were dispersed into
140 50 mL of deionized water. The pH of the suspension was controlled at the range of 2.5-3.0 by
141 0.1 mol/L HCl solution. Before titration, the suspension was purged with an N₂ atmosphere at
142 25°C for 30 min. The suspension was titrated by 0.1 mL standardized 0.1 mol/L NaOH with 60
143 s intervals until the pH value reached 11, the electrical conductivity and the volume of NaOH
144 were recorded for the calculation of the total carboxyl content.³³

145 The copper number was determined according to Tappi standard method (T 430 cm-09).
146 The carbonyl content was linear correlated with the copper number and calculated by the
147 following equation:³⁴

$$CCOA = \frac{(Cu\# - 0.07)}{0.06} \quad (2)$$

148
149 Where CCOA represents the total carbonyl content of SB (mmol/kg) and Cu# represents
150 the copper number (%).

151 **XPS analysis.** Before XPS analysis, ozone-treated SB was extracted by dichloromethane to
152 remove the extractives according to standard Tappi T 204 cm-07. XPS analysis was performed

153 by X-ray Photoelectron Spectroscopy (Axis Ultra DLD, Kratos Analytical, UK) using a
154 monochromated Al K α source (5mA, 15kV). For the high-resolution spectra, the analytical area
155 was 0.7 mm \times 0.3 mm with a pass energy of 40 eV. All samples were tested three times. All
156 spectra were fitted by XPS peak 4.1 using Lorentzian-Gaussian line shape (20% Lorentzian
157 contribution) after Tougaard background correction.

158 The surface lignin ($\emptyset_{\text{Lignin}}$) of SB was calculated by the O/C ratios based on the XPS
159 spectrum (Eq. 3)³⁵. The calculated equation is as follows:

$$\emptyset_{\text{Lignin}} = \frac{O/C_{(\text{sample})} - O/C_{(\text{lignin-free SB})}}{O/C_{(\text{lignin})} - O/C_{(\text{lignin-free SB})}} \quad (3)$$

160 Where O/C (sample) is the O/C ratio of the SB sample after extraction, O/C (lignin) is the
161 O/C value of lignin (0.33).³⁶ The theoretical O/C value of cellulose is 0.83, the O/C value of
162 the hemicellulose of SB is approximately 0.8,^{37, 38} and the O/C value of delignified pulp is
163 0.8.³⁹

164 Herein, the O/C (lignin-free SB) value of 0.8 was used in the equation to represent the
165 lignin-free of SB.

166 **Determination of MB adsorption.** 200 mL of 100 mg/L MB solution was shaken with 1 g
167 of SB using an air-bath shaker (200 rpm) at 30°C. The pH of the initial solution was 6.0 adjusted
168 by 0.1 N HCl solution and 0.1 N NaOH solution. The concentration of residual MB was
169 examined at different time intervals using a UV-VIS spectrophotometer (UV-2600, Shimadzu,
170 Japan) at the wavelength of 665 nm. A standard calibration curve was built by different
171 concentrations of MB solution (0, 1, 2, 3, 4, 5 mg/L) with a linear correlation coefficient of
172 0.999. The adsorbed MB was calculated as the following equation:

$$Q = \frac{(C_0 - C)V}{M} \quad (4)$$

173

174 Where Q represents the content of adsorbed MB (mg/g); V represents the volume of the
175 solution (L); C_0 represents the initial concentration of MB (mg/L); C represents the
176 concentration of MB (mg/L), and M represents the mass of the sample (mg). The equilibrium
177 concentration of the residual MB was examined after 24 hours of adsorption.

178 **Determination of adsorption of PDADMAC.** The adsorption capability of SB towards
179 PDADMAC was determined using a particle charge detector (PCD-03 pH, Müttek™, Germany).
180 0.1 g milled sample was dispersed in 10 mL deionized water and titrated by 0.001 N
181 standardized PDADMAC solution. The adsorption capability was calculated as the following
182 equation:

$$q = \frac{c * V}{m} \quad (5)$$

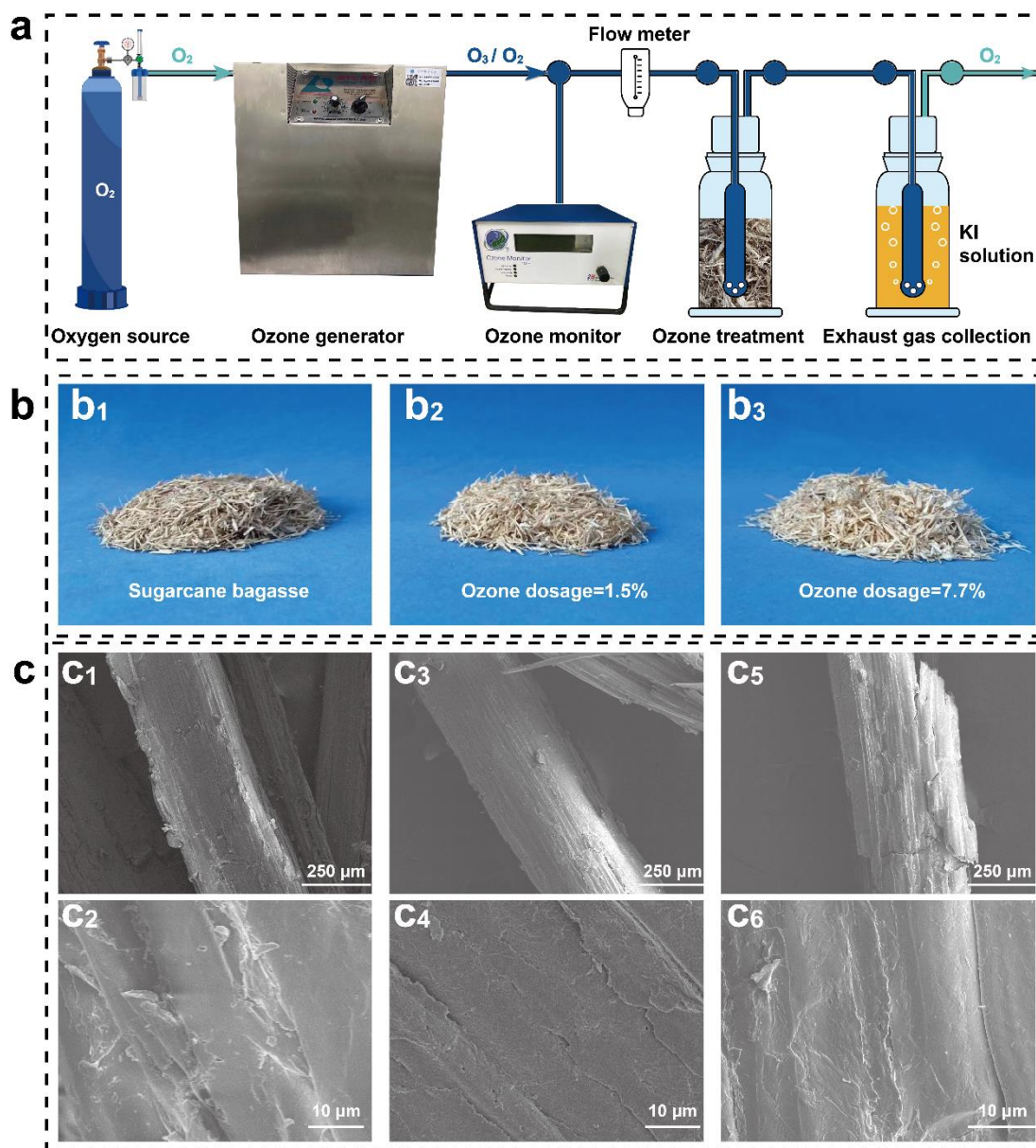
183 Where q represents the adsorption capability of SB towards PDADMAC (mmol/kg); V
184 represents the volume of PDADMAC used (ml); c represents the concentration of PDADMAC
185 (mmol/ml), and m represents the weight mass of the sample (kg).

186 **Results and discussion**

187 **Ozone modification of SB.** Ozone modification we developed was green and sustainable
188 without requiring harsh reaction conditions (high temperature and pressure), toxic chemicals,
189 and high chemical load. Besides, the original shape and size of SB were also maintained,
190 thereby ensuring that the modified SB could be easily recycled. The detailed ozone
191 modification process of SB was illustrated in Figure 2a. Under normal temperature and

192 pressure, a continuous flow of ozone with a concentration of 150~170 g/m³ produced by the
193 ozone generator entered the gas-washing bottle containing 10 g SB at the flow rate of ~1.5
194 L/min. The total ozone consumption was between 1.5~7.7% of the weight of SB. After the
195 ozone treatment, there was no significant change in the morphology of SB at the macro scale,
196 but the color became lighter (Figure 2b₁~2b₃), which could be due to the decrease of the lignin
197 content and the chromogenic groups in SB. Lignin is rich in the chromophore groups and
198 therefore is the main color source of most lignocellulosic biomass. Ozone could effectively
199 cleave the chromophore groups of lignin and further oxidize them to carboxyl or aldehyde
200 groups, resulting in a decrease in the polymerization degree (DP) and an increase in the
201 solubility of the lignin, which ultimately lead to the decreased lignin content and chromophore
202 groups in SB.⁹

203 To investigate the effects of ozone on the microstructure of SB, the SB before and after
204 ozone modification were characterized by SEM. As can be seen from Figure 2c₁, 1c₃, and 1c₅,
205 similar to the macrostructure, the microstructure of SB was also basically maintained. While
206 the chemical compositions of the SB surface had undergone major changes (Figure 2c₂, 1c₄,
207 and 1c₆), which played an important role in the adsorption rate. As shown in Figure 2c₂, the
208 surface of the original SB was covered by melted substances, which could be composed of
209 lignin.¹⁰ When the ozone consumption was 1.5 wt%, the surface of ozone-modified SB (Figure
210 2c₄) had significantly fewer melted substances, but the melted substances could be clearly
211 observed again when the ozone consumption attained 7.7 wt% (Figure 2c₆). This revealed that
212 the partially dissolved lignin modified by ozone could re-deposit onto the surface of SB due to
213 the increase in pH during the washing process.¹⁰



214

215 **Figure 2** (a) Schematic image of ozone modification process. (b) Photos showing original

216 SB (b₁) and ozone-modified SB with an ozone consumption of 1.5 wt% (b₂) and 7.7 wt% (b₃).

217 (c) SEM images of original SB (c₁ and c₂) and ozone-modified SB with an ozone consumption

218 of 1.5 wt% (c₃ and c₄) and 7.7 wt% (c₅ and c₆).

219 **Effects of ozone on the compositions and functional groups of SB.** To improve the

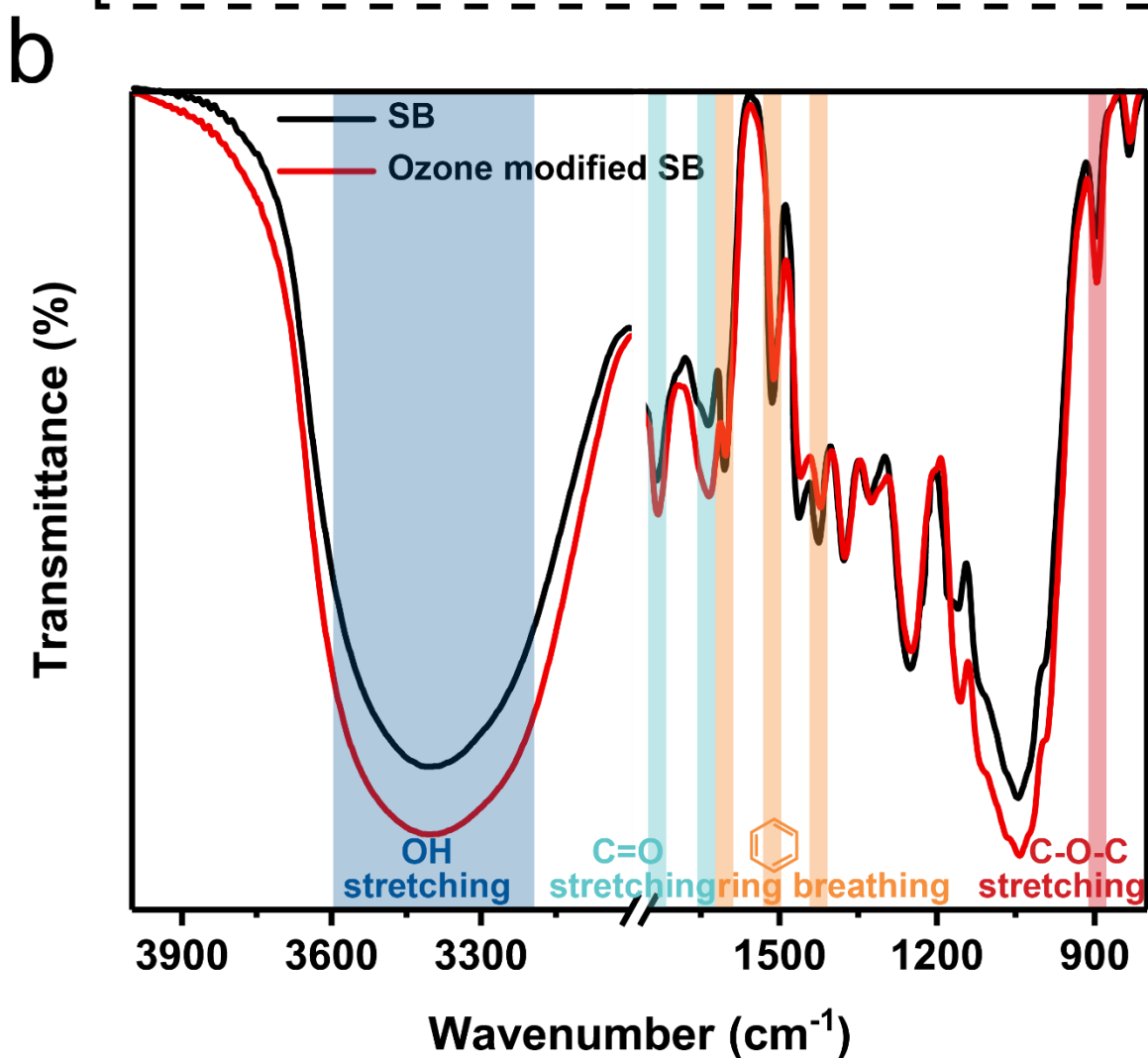
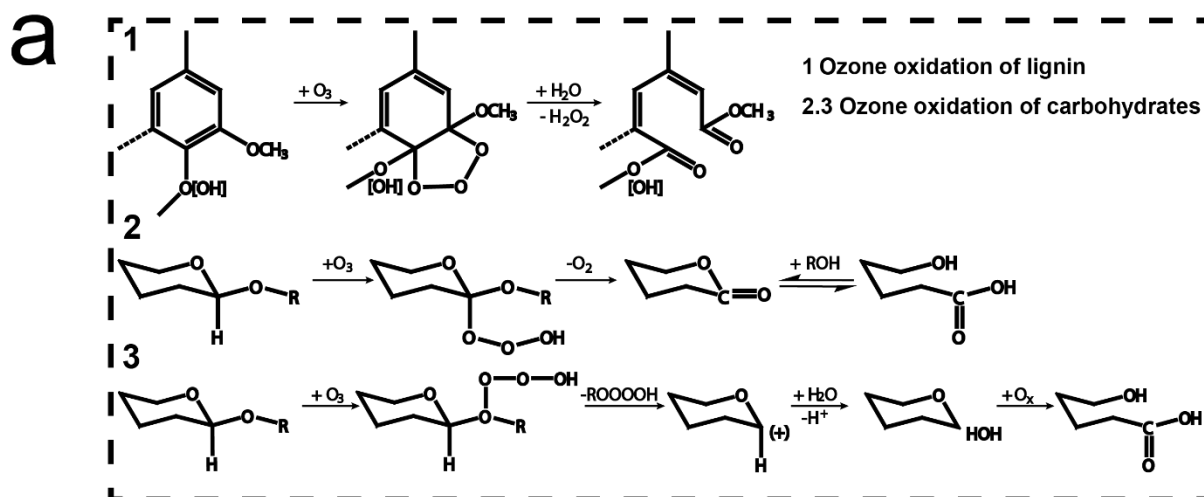
220 adsorption capability of SB towards cationic organic pollutants, ozone modification was used

221 to increase its carboxyl content. Figure 3a₁-a₃ showed the ozone modification towards the three

222 main components (cellulose, hemicellulose, and lignin) in SB. For lignin, ozone has high
223 reactivity and selectivity to its aromatic and olefinic structures. Ozone first reacts with the
224 double bonds in lignin through 1,3-dipolar addition to form primary ozonide, which is then
225 hydrolyzed into muconic acid derivatives (containing carbonyl and carboxyl groups) and
226 hydrogen peroxide (Figure 3a₁).⁹ Moreover, with the further increase in ozone consumption,
227 the aromatic structures and double bonds of the side chains of lignin would be cleaved to small
228 molecules of high hydrophilic fatty acids, causing partial removal of lignin from the SB.⁹ For
229 carbohydrates (cellulose and hemicellulose), ozone can directly attack the glycosidic bonds to
230 form hydrogen trioxide, which was then cleaved to form lactone and oxygen. Finally,
231 carbohydrates were hydrolyzed to form a carboxyl-containing structure (Figure 3a₂ and 3a₃).⁹

232 To further investigate the effects of ozone modification towards the compositions and
233 functional groups of SB, Fourier Transform Infrared Spectroscopy (FTIR) was used (Figure
234 3b). Regarding the change of functional groups, after ozone modification, the adsorption bands
235 at 1637 cm⁻¹ and 1735 cm⁻¹ assigned to the C=O stretching of carboxylate (-COO⁻) and free
236 carboxyl groups (-COOH) were strengthened, which confirmed the effects of ozone on
237 increasing the carboxyl groups of SB. Regarding the change of compositions, it can be seen
238 that the absorbance peaks at 1425 cm⁻¹, 1514 cm⁻¹, and 1604 cm⁻¹ assigned to the ring breathing
239 vibrations of benzene in lignin structure were weakened after ozone modification. Meanwhile,
240 the absorbance peak at 897 cm⁻¹ assigned to the C–O–C stretching vibration of glycosidic bond
241 of carbohydrates (cellulose and hemicellulose) was strengthened. This indicated that ozone
242 exhibited high selectivity to aromatic structures of lignin than the glycosidic bonds of
243 carbohydrates. Besides, due to the decrease content of the lignin, the SB exhibited more

244 hydroxyl groups (3406 cm^{-1} OH stretching vibration strengthened) after ozone modification.
245 Overall, ozone can react with all the three main components in SB to generate carboxyl-
246 containing derivatives, indicating the high feasibility of using ozone to improve the adsorption
247 capability of SB towards cationic organic pollutants.



248

249 **Figure 3** (a) Ozone modification reaction towards the three main components (cellulose,

250 hemicellulose, and lignin) of SB. (b) FTIR spectrum of SB before (black line) and after ozone

251 modification (1#, red line).

252 **Composition analysis of SB before and after ozone modification.** Composition analysis
253 could directly show the effects of ozone modification on the cellulose, hemicellulose, and
254 lignin of SB. The changes of the three main chemical components of SB with the ozone
255 consumption were illustrated in Figure 4a. Since ozone is an effective reactant, the contents of
256 all three components decreased with the increase of ozone consumption. When the ozone
257 consumption was only 1.5 wt% (Sample 1), the yield of ozone-modified SB was as high as
258 95.9%, the total lignin decreased about 21.9%, whereas the cellulose and hemicellulose
259 decreased only about 1.7 wt% and 0.19 wt%, respectively. As the ozone consumption reached
260 to 7.7 wt% (Sample 4), a high yield (88.4%) was still obtained, the decrease of total lignin
261 slowed down (33% decrease) but the decrease of cellulose and hemicellulose increased (3.8 %
262 for cellulose and 6.1% for hemicellulose).

263 Ozone showed high selectivity to lignin, especially when the lignin content of SB was high
264 (Figure 4b). That was because ozone has higher reactivity towards aromatic and side-chain-
265 olefin of the lignin structure⁹ than the glycosidic bonds of carbohydrates. The selectivity of
266 ozone towards lignin decreased quickly as the decrease of total lignin content. Meanwhile, the
267 selectivity of ozone towards cellulose and hemicellulose increased quickly (Figure 4b). This
268 indicated that the oxidation tended to occur on the surface of SB rather than inside the SB due
269 to its compact structure, despite the presence of lots of pores. Once the lignin on the surface
270 was reduced to some extent, the oxidation of the cellulose and hemicellulose exposed from the
271 covered lignin would increase, thus causing the rapid weight loss of carbohydrates (cellulose
272 and hemicellulose). In addition, according to Ben, et al., the hydroxyl contents of cellulose,

273 hemicellulose, and lignin were about 18.52 mmol/g, 14.43 mmol/g, and 5.29 mmol/g,
274 respectively.¹¹ The high weight loss of lignin and low weight loss of cellulose and
275 hemicellulose indicated that the relative content of the hydroxyl group in ozone-treated SB
276 increased, which was beneficial to increase the hydrophilic properties of SB and therefore
277 improve the adsorption rate of SB.

278 Interestingly, compared to the original SB, only acid-insoluble lignin in total lignin
279 decreased, while acid-soluble lignin increased during the ozone modification. The increased
280 acid-soluble lignin value remained constant after the ozone consumption reached 1.5 wt%
281 (sample 1). This could be attributed to the decrease of DP of acid-insoluble lignin and the
282 increase of carboxyl groups, which transformed acid-insoluble lignin into acid-soluble lignin.¹⁰
283 Acid-soluble lignin would be further oxidized to small molecule acids or even to carbon
284 dioxide and water.⁹ The constant value of acid-soluble lignin could be due to the balance
285 between the oxidation of acid-insoluble lignin and acid-insoluble lignin. Additionally, the
286 increase of acid-soluble lignin also meant the increase of carboxyl groups of lignin in SB.

287 It can be concluded from above that ozone showed high selectivity towards lignin and
288 increase the functional groups of SB with low ozone consumption. The increase of functional
289 groups in SB, including hydroxyl and carboxyl groups, could be benefited for its adsorption
290 abilities in terms of adsorption capability and adsorption rate. To further find out the effects of
291 ozone on the functional groups of ozone-treated SB, the total and surface functional groups
292 (carboxyl and carbonyl groups) were tested.

293 **Characterization of functional groups in the ozone modified SB.** The contents of

294 carbonyl and carboxyl groups are important parameters reflecting the reaction behavior of
295 ozone to SB and the potential of ozone modification for anionic groups increase. The change
296 of total carbonyl and carboxyl groups with the ozone consumption was illustrated in Figure 4c
297 and 4d. After ozone modification, both the contents of carboxyl and carbonyl groups increased.
298 The carboxyl groups increased first and then tended to gentle as the increase of ozone
299 consumption. Meanwhile, the carbonyl groups increased first and then slightly decreased with
300 the increase of ozone consumption. This change could be closely related to the composition
301 change during the ozone modification. Before ozone consumption attained at 3.01 wt%
302 (Sample 1 and Sample 2), the increase of carboxyl and carbonyl groups was accompanied by
303 the rapid decrease of lignin content (Figure 4a). A certain amount of carbonyl and carboxyl
304 groups were formed through the reaction of ozone with the olefin and aromatic structures of
305 lignin.¹²

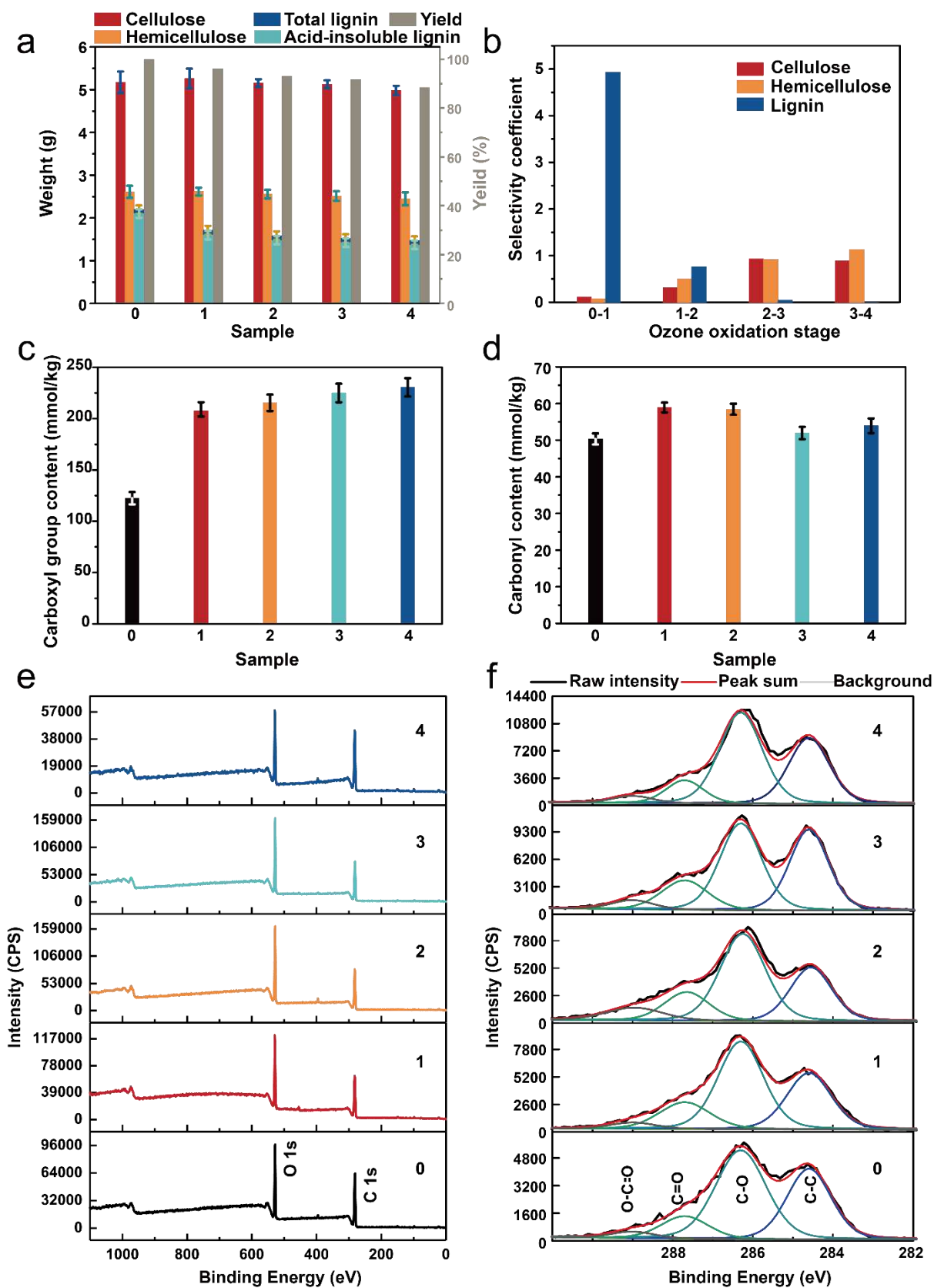
306 When ozone consumption was beyond 3.01 wt% (Sample 3 and Sample 4), the composition
307 change was dominated by the degradation of carbohydrates, thus causing the corresponding
308 changes of functional groups (Figure 4a). This process can be divided into three steps¹³: the
309 formation of carbonyl groups, followed by oxidation to carboxyl groups, and
310 decarboxylation.¹⁴ The reason for the steady-state of carboxyl content could be that the rate of
311 oxidation of the carbonyl groups to carboxyl groups was approximately equal to that of
312 decarboxylation.¹⁴ Importantly, the total carboxyl and carbonyl groups were increased about
313 84.1% and 16.1% (Sample 1) with an ozone consumption of only 1.5 wt%. Overall, ozone
314 modification effectively increased the total content of carboxyl groups of SB under the
315 conditions of high yield and low ozone consumption.

316 The surface chemical properties (including compositions and functional groups) have
317 significant effects on its physicochemical properties and are the important factors for the
318 adsorption rate from dilute aqueous solutions.¹⁵⁻¹⁷ XPS analysis were used to determine the
319 carboxyl and carbonyl contents on the surface of extractives-free SB (Figure 4e and 4f). The
320 XPS analysis of extractives-free SB revealed four C peaks at 284.6, 286.3, 287.9, and 288.2
321 eV (Figure 4f), originating from C1 (C-C), C2 (C-O), C3 (O-C-O and/or C=O), and C4 (O-
322 C=O), respectively.¹⁸ Carbohydrates exhibited two peaks in the XPS spectrum, C2 (alcohols
323 and ethers), and C3 (ketones and aldehydes). The peak C1 (aliphatic carbon) only originated
324 from the lignin of extractives-free SB, because the extractives have been removed by extraction
325 and C-C bonds do not exist in the carbohydrates (cellulose and hemicellulose).

326 The relative intensities of four peaks, O/C ratios, and the calculated surface lignin contents
327 of the ozone-treated SB with different ozone consumption were shown in Table 1. Unlike the
328 decrease of the total lignin content, the content of surface lignin first decreased and then
329 increased with the increase of the ozone consumption. According to the results of composition
330 analysis, there were two stages in the ozone modification process, namely rapid weight loss of
331 lignin and rapid weight loss of carbohydrates. Similar stages could also exist for the surface
332 composition of SB. Since $\emptyset_{\text{Lignin}}$ is the relative content of lignin, the decrease of $\emptyset_{\text{Lignin}}$ could
333 be mainly due to the partial dissolution of the lignin during the first stage. The increase of
334 $\emptyset_{\text{Lignin}}$ could be due to the abovementioned degradation of carbohydrates during the second
335 stage and the increased content of re-deposited lignin. According to the results of component
336 analysis, the content of dissolved lignin in the system increased with the ozone consumption,
337 resulting in an increase in the content of re-deposited lignin, which was consistent with the

338 SEM results.

339 The change of carboxyl groups on the surface of SB can be indicated by the relative
340 intensity of C4 (carboxylic acid and ester). In Table 1, both the content of carbonyl and carboxyl
341 groups first increased and then decreased with the increase of ozone consumption. This result
342 could be closely related to the carboxylation reaction of ozone and the surface composition
343 change of SB. The carboxylation reaction of ozone towards all three components could
344 significantly increase the carboxyl groups of SB and decrease the content of surface lignin.
345 The subsequent decrease could be due to the redeposition of dissolved lignin with a certain
346 carboxyl content. The carboxyl groups on the SB surface increased dramatically during the
347 ozone modification with a maximum increase of 257% at the ozone consumption of 3.0 wt%.
348 When the ozone consumption reached 7.7 wt%, the carboxyl groups still increased about 132%.
349 Overall, after ozone treatment, the surface of SB contains increased anionic groups (carboxyl
350 groups) and less hydrophobic lignin to expose the abundant hydroxyl groups, which could be
351 beneficial to its adsorption rate.



352

353 **Figure 4** (a) Effects of different ozone consumption on the chemical compositions of ozone-

354 treated SB. (b) Selectivity coefficient change with ozone consumption. Effects of ozone

355 consumption on the total carboxyl (c) and carbonyl groups (d) of the ozone-treated SB. The
 356 XPS spectra of extractives-free ozone-treated SB with different ozone consumption. (e) full
 357 survey, (f) C 1s high resolution XPS spectra.

358 **Table 1** XPS analysis of the extractives-free ozone-treated SB with different ozone
 359 consumption.

Sample	Ozone consume charge (%)	O/C	Binding energy (eV)				Ø Lignin (%)
			C1 (%) C-C 284.6	C2 (%) C-O 286.3	C3 (%) C=O 287.9	C4 (%) O-C=O 288.2	
0	0.0	0.50	35.6	49.6	12.0	2.8	65
1	1.5	0.59	30.2	51.2	14.2	4.3	48
2	3.0	0.60	26.4	48.8	14.8	10.0	47
3	4.4	0.56	36.6	46.1	11.1	6.3	55
4	7.7	0.52	34.4	47.1	12.1	6.5	61

360

361 **Adsorption of cationic organic pollutants by ozone-modified SB.** To investigate the
 362 adsorption abilities of the ozone-modified SB towards cationic organic pollutants (Figure 5a),
 363 batch adsorption experiments were carried out by using 1 g of ozone-modified SB in 200 mL
 364 of 100 mg L⁻¹ MB solution with a pH of 6 at 30°C. As illustrated in Figure 5b, the adsorption
 365 of MB can be divided into three stages, namely the rapid adsorption period, slow adsorption
 366 period, and the equilibrium adsorption period.^{19, 20} The above three stages were controlled by
 367 film diffusion, intraparticle diffusion, and the physisorption and chemisorption, respectively.
 368 During the adsorption process, MB molecules first diffused from the solution to the external
 369 surface of the adsorbent (film diffusion), then migrated to the interior surface (intraparticle
 370 diffusion), and finally adsorbed on the surface sites of SB (physisorption or chemisorption).^{19,}
 371 ²¹ By increasing the hydrophilic groups (hydroxyl and carboxyl groups) and cation adsorption

372 sites (carboxyl groups) of SB, the ozone-modified SB exhibited a higher adsorption rate,
373 especially at the early stage of adsorption, as well as a higher adsorption capacity than that of
374 the original SB (Figure 5b). Furthermore, according to the results of adsorption equilibrium
375 experiments (listed in Table 3), among all the ozone-modified SB, Sample 1 exhibited the
376 largest adsorption capability of 9.237 mg/g SB, 11.3% higher than the original SB (8.295 mg/g
377 SB), and largest adsorption rate of 0.624 mg·g⁻¹·min⁻¹ after 10 minutes of contact with MB,
378 33.3% higher than original SB (0.416 mg·g⁻¹·min⁻¹). As the ozone consumption charge further
379 increased, both the maximum adsorption rate and adsorption capacity of SB slightly decreased.

380 To reveal the mechanism of the ozone-modified SB participating in the MB adsorption
381 process, three kinetic models were adopted, namely irreversible first-order, reversible first-
382 order, and pseudo-second-order models (Table 2). The irreversible first-order model is derived
383 as the assumption that once adsorbed, the particle cannot diffuse along or desorb from the
384 surface. From Figure 5c, the irreversible first-order model only fitted well at the first 20~30
385 min of the adsorption process instead of the whole adsorption process, indicating the adsorption
386 is dominated at the initial stage of adsorption rather than desorption. The reversible first-order
387 model is derived under the assumption that the adsorption and desorption rate constants are
388 equal to the equilibrium reaction rate constant.^{22, 23} As for the pseudo-second-order model,
389 which is contrary to the previous models, it assumes the “chemisorption” behaviour over the
390 whole biosorption process.²⁴

391 From Figure 5c~e and Table 3, compared to the other two models, pseudo-second-order
392 model is the best fitted model for both original and ozone-modified SB with a R² higher than
393 0.990. In addition, since the nonlinear regression method is believed to be more appropriate for

394 determining the rate kinetic parameters,^{25,26} nonlinear pseudo-second-order kinetic model was
395 also adopted in this study (Table 2). As shown in Figure 5f, the non-linear pseudo-second-order
396 kinetic plots correlated well with the experimental data ($R^2 > 0.990$). The related adsorption
397 parameters (k_{II} and q_e , Table 3) were very close to that of linear pseudo-second-order model
398 (k_{II} and q_e) and the experimental data (q_e), which further confirmed that the pseudo-second-
399 order model could be suitable for investigating the adsorption mechanisms of SB towards MB.
400 This indicated that the adsorption of MB by SB was more like the chemisorption-based process
401 involving ions exchange between cationic MB and functional groups (mainly -OH and -COOH)
402 of SB.²⁷⁻²⁹ Besides, instead of relying on the assumption that the rate-limiting step is the film
403 diffusion, the rate-limiting step of the pseudo-second-order kinetic model assumed is
404 chemisorption.²⁸ Therefore, the change of maximum adsorption rate (MAR) and capacity could
405 be closely related to the change of functional groups during the ozone modification.

406 The MAR changes of different ozone-modified SB with the increase of ozone
407 consumption correlated well with the changes of hydroxyl and carboxyl groups on its surface,
408 which can be indicated by O/C ratios and C4 relative intensity in Table 1. Since MAR was
409 reached at the film diffusion stage, the increased hydrophilic hydroxyl and carboxyl groups on
410 the surface could enhance the hydrophilicity, thereby promoting the permeation of water as
411 well as the MB molecules through the film, and finally increasing the MAR.³⁰ Meanwhile, the
412 change of adsorption rate also showed a similar trend. The increase of the carboxyl group
413 content could lead to the increased chemisorption sites for cationic organic pollutants, which
414 in turn increased the cationic adsorption capacity of ozone-modified SB. Therefore, the reason
415 for the decrease of adsorption capability could be that the redeposited lignin as one of the

416 important sources of adsorption sites (carboxyl groups) for MB could redissolve into the
 417 solution during the adsorption process, which therefore reduced its adsorption capability.

418 **Table 2** Mathematical expressions of the three kinetic models.

Kinetic model	Equation	Integrated form
Irreversible first-order	$dq/dt = k_1(Q_e - Q)$	$\log(Q_e - Q) = \log q_e - (k_1/2.303)t$
Reversible first-order	$dc/dt = k_1C - k_{-1}X$	$-\ln((C - C_e)/(C_0 - C_e)) = kt$
Pesudo-second-order	$dq/dt = k_{II}(Q_e - Q)^2$	$t/Q = 1/(k_{II}q_e^2) + t/q_e$
Non-linear Pesudo-second-order	$dq/dt = k_{II}(Q_e - Q)^2$	$Q = k_{II}q_e^2t/(1 + k_{II}q_e^2t)$

419 Where t is the adsorption time (min), q is the amount of MB adsorbed per unit of SB at
 420 time t (mg/g), k_1 is the rate constant for first-order kinetic model (min^{-1}), Q is amount of MB
 421 adsorbed per unit of SB at time t (mg/g), Q_e is the experimental amount of MB adsorbed per
 422 unit of SB (mg/g), q_e is the calculated amount of dye molecules adsorbed per unit of SB (mg/g),
 423 k_1 is the forward reaction rate constant, k_{-1} is the reverse reaction rate constant, k is the
 424 equilibrium rate constant for e reversible kinetic model (equal to the ratio of k_1 to k_{-1}), c is the
 425 initial concentration of MB at time t (mg/L), X is the MB in the solid phase, C_0 is the initial
 426 concentration of MB (mg/L), C_e is the equilibrium concentration of MB (mg/L), C is the
 427 concentration of MB (mg/L) at time t , k_{II} is the rate constant of pseudo-second-order kinetic
 428 model ($\text{g mg}^{-1} \text{min}^{-1}$).

429 **Table 3** Kinetic rate constant related to the biosorption of MB onto ozone modified SB.

	Sample				
	0	1	2	3	4
Irreversible first-order					
k_I	0.033	0.042	0.033	0.029	0.030
Calculated q_e	3.857	4.452	2.923	2.924	3.560
R^2	0.998	0.841	0.983	0.927	0.977
Reversible first-order					
K	0.045	0.033	0.027	0.030	0.041

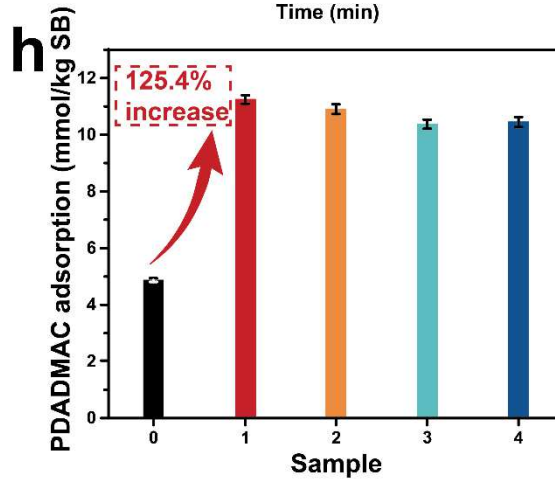
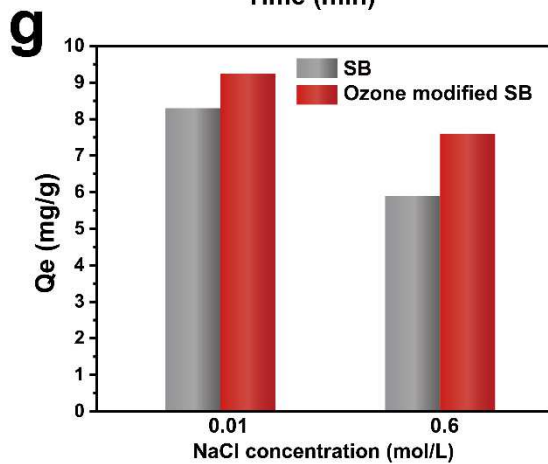
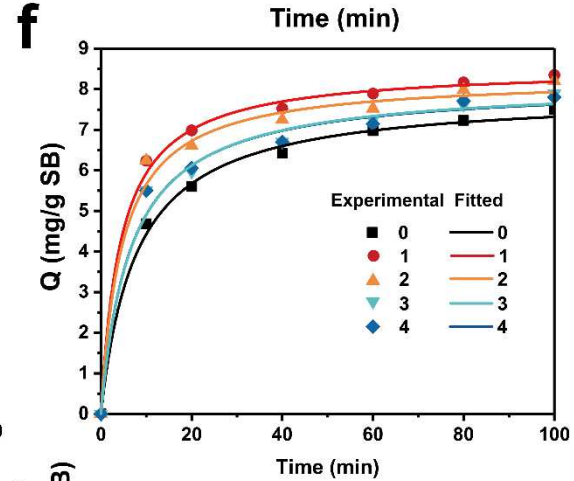
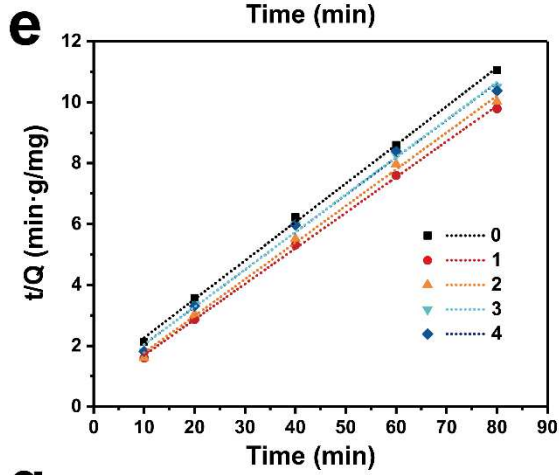
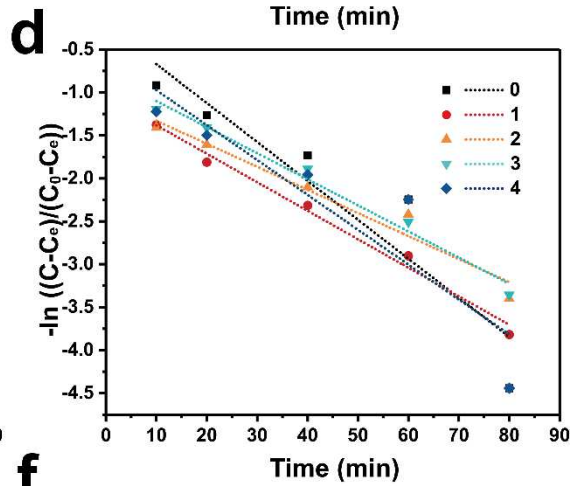
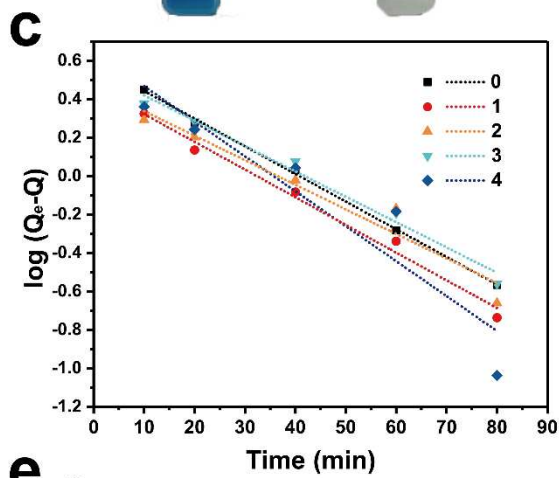
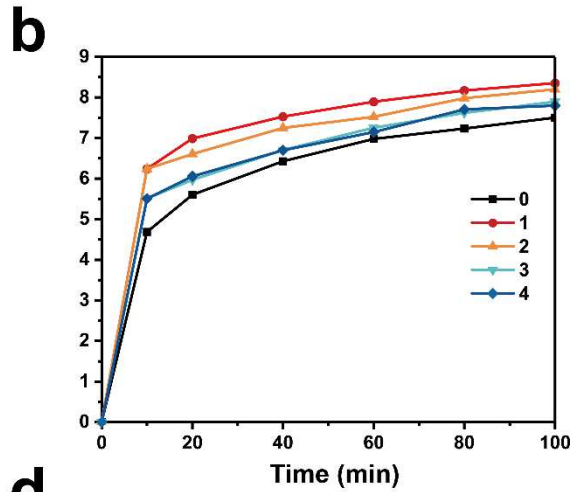
R^2	0.827	0.983	0.942	0.977	0.775
Pesudo-second-order					
k_{II}	0.016	0.027	0.026	0.019	0.019
Calculated q_e	7.886	8.540	8.295	8.117	8.143
R^2	0.999	0.999	0.997	0.996	0.994
Non-linear Pesudo-second-order					
k_{II}	0.016	0.027	0.026	0.019	0.019
Calculated q_e	7.886	8.540	8.295	8.117	8.143
R^2	0.997	0.998	0.992	0.990	0.991
Experimental q_e	8.295	9.237	9.063	8.725	8.613

430 Where R^2 is the squared regression correlation coefficient.

431 When removing cationic pollutants from the ocean, it is important to consider the effect
432 of NaCl concentration on the adsorption performance of adsorbent because the seawater
433 contain a high concentration of salt (~0.6 M NaCl solution). Figure 5g showed the effect of the
434 NaCl concentration on the adsorption capability of the SB and ozone modified SB (Sample 1)
435 towards MB. Both the adsorption capability of SB and ozone modified SB decreased as the
436 NaCl concentration increased, which could be due to the competitive effects between the Na^+
437 and MB ions on the sites available for sorption. In addition, after ozone modification, the
438 increased available sorption sites made the ozone modified SB more resistant to salt water than
439 the original SB. The adsorption capability of original SB in 0.6M NaCl solution decreased 29.0%
440 than in 0.01M NaCl, while ozone modified SB only decreased 17.7%.

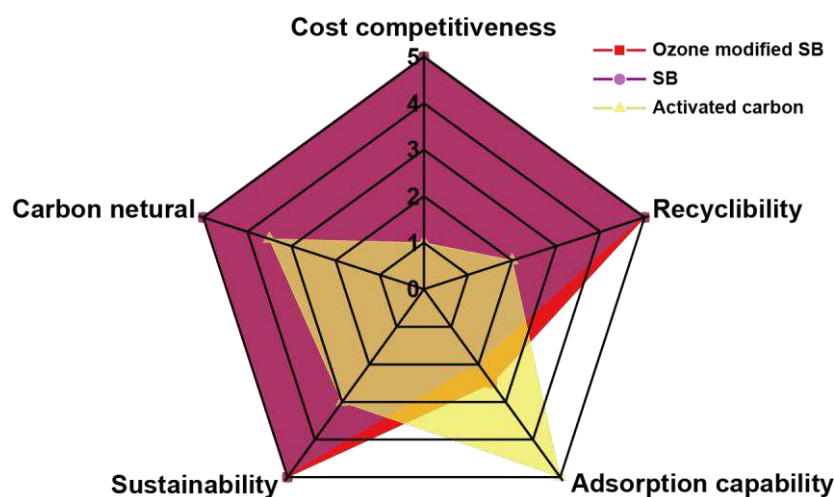
441 To evaluate the adsorption performance of ozone-modified SB towards cationic polymers
442 with high charges (for example, cationic polyelectrolytes), batch adsorption experiments were
443 conducted by using 0.1 g milled ozone modified SB to adsorb the 0.001 N cationic PDADMAC.
444 As shown in Figure 5h, the adsorption capability of ozone-modified SB first increased sharply,
445 and then slightly decreased with the increase of the ozone consumption. The adsorption
446 capacity of PDADMAC increased to 125.4% when the ozone consumption was only 1.5 wt%

447 (Sample 1). This result was consistent with the change in MB adsorption capacity and the total
448 carboxyl groups. Negatively charged functional groups (carboxyl groups) played an important
449 role during the adsorption of PDADMAC. Since the pKa of carboxylic groups were about 5.4,
450 the carboxylic groups can dissociate into anionic groups at neutral pH. The increase of
451 negatively charged carboxyl groups on the SB could increase the PDADMAC adsorption
452 because of the existence of chemical reactions or cation exchange between them.^{31,32} Therefore,
453 the increase of carboxyl groups by ozone modification can effectively increase the PDADMAC
454 adsorption of SB.



456 **Figure 5** Adsorption of cationic organic pollutants by the ozone modified SB. (a) Schematic
457 diagram of adsorption of cationic organic pollutants by the ozone modified SB, (b) the
458 adsorption curves for MB onto the ozone modified SB (SB concentration=5 g/L, initial solution
459 pH = 6, temperature = 30°C), linear irreversible first-order (c), reversible first-order (d),
460 pseudo-second-order (e), and non-linear pseudo-second-order (f) kinetic plots of MB
461 adsorption onto different ozone modified SB, (g) effect of NaCl concentration (0.01 M and 0.6
462 M) on the adsorption capability of SB and ozone modified SB (Sample 1), (h) adsorption
463 capacity of PDADMAC onto the different ozone modified SB.

464 **Comparison with other adsorbents.** Compared with the current commercial activated
465 carbon, SB, as the agro-industrial wastes and by-products has outstanding advantages in terms
466 of carbon neutral, sustainability, cost efficiency, and recyclability (Figure 6). To improve the
467 limited adsorption capability towards cationic pollutants and maintain its above advantages,
468 this study uses ozone to make simple and green modification of SB. After ozone modification,
469 the adsorption capacity of SB for cationic pollutants was efficiently improved with low ozone
470 consumption, the morphology of bagasse was maintained to ensure its good recyclability, and
471 the degraded lignin and carbohydrates could be biodegraded to ensure its sustainable
472 performance. Furthermore, compared with other modification methods that require high
473 chemical dosage, expensive chemical cost, and high process cost, the amount of ozone used
474 for modification is 15 kg/ton sugarcane bagasse with a cost of only \$72/ ton.



475

476 **Figure 6** Radar chart showing cost efficiency, recyclability, carbon neutral, sustainability, and
 477 good adsorption capability of ozone modified SB, compared to original SB and activated
 478 carbon.

479 **Conclusion**

480 In this study, SB was successfully modified by ozone at normal pressure and temperature.
 481 High yield (95.9%), low lignin content (21.9% total lignin removals), and high content of
 482 functional groups containing SB was obtained with only 1.5 wt% ozone consumption. The total
 483 content of carboxyl groups as the main adsorption sites for cationic organic pollutants was
 484 increased by about 84.1%. The increase of the functional groups and reduction of the lignin
 485 coverage by ozone modification increased the adsorption abilities of SB. The maximum
 486 adsorption rate and capacity of SB for MB were increased by about 33.3% and 11.3%,
 487 compared to the original SB. Besides, ozone modified SB maintained its high adsorption
 488 capability even at high NaCl concentration (0.6 M). For cationic polymer with high charges
 489 (PDADMAC), the adsorption capacity of the milled SB increased about 125.4%. A further
 490 increase in the ozone consumption, however, would not increase the adsorption abilities but

491 could decrease the yield. Considering ozone as an efficient and green reactant, ozone
492 modification is believed to be a promising method for increasing the adsorption abilities of
493 lignocellulosic materials towards cationic organic pollutants.

494 Acknowledgments

495 This research was supported by the Guangzhou Science and Technology Plan Projects
496 (NO. 201707020011), the National Science and Technology Major Project (NO.
497 2017ZX07402004), the State Key Laboratory of Pulp and Paper Engineering (NO. 201831),
498 and Guangdong Province Science Foundation for Cultivating National Engineering Research
499 Center for Efficient Utilization of Plant Fibers (NO. 2017B090903003).

500

501 Reference

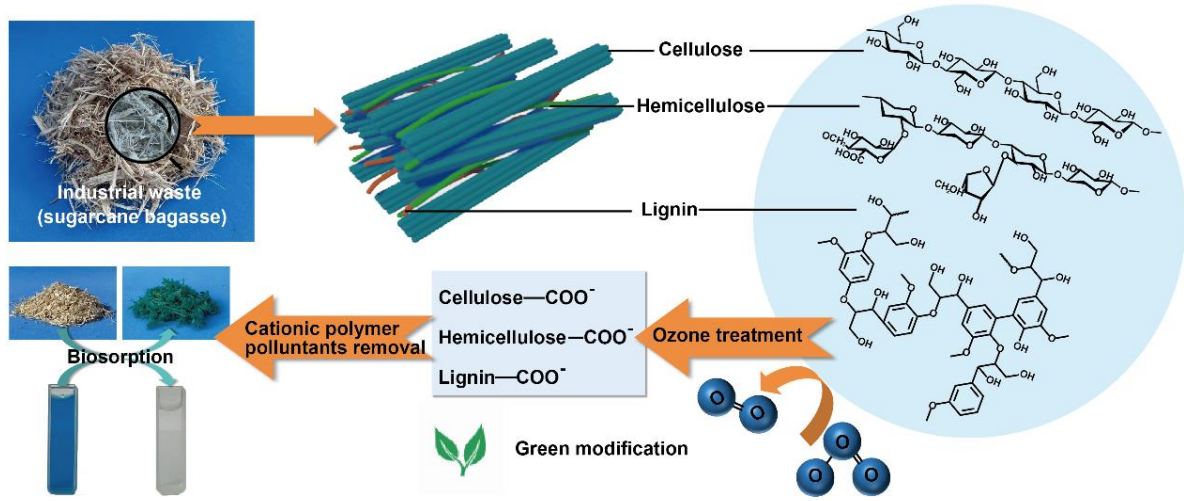
- 502 (1) Guillen, J.; Natale, F.; Carvalho, N.; Casey, J.; Hofherr, J.; Druon, J.-N.; Fiore, G.; Gibin, M.; Zanzi, A.;
503 Martinsohn, J. T. Global seafood consumption footprint. *Ambio* **2019**, *48* (2), 111-122.
- 504 (2) Livingstone, D.; Gallacher, S. Contamination and Spoilage of Molluscs and Crustaceans. In *Encyclopaedia*
505 *of Food Sciences and Nutrition*; Academic Press: Boston, 2003; pp 5228-5245.
- 506 (3) Zhou, Y.; Lu, J.; Zhou, Y.; Liu, Y. Recent advances for dyes removal using novel adsorbents: a review.
507 *Environ. Pollut.* **2019**, *252*, 352-365.
- 508 (4) Gupta, V. K.; Ali, I.; Saleh, T. A.; Nayak, A.; Agarwal, S. Chemical treatment technologies for waste-water
509 recycling—an overview. *RSC Adv.* **2012**, *2* (16), 6380-6388.
- 510 (5) Aksu, Z. Application of biosorption for the removal of organic pollutants: a review. *Process Biochem.* **2005**,
511 *40* (3-4), 997-1026.
- 512 (6) Yan, J.; Oyediji, O.; Leal, J. H.; Donohoe, B. S.; Semelsberger, T. A.; Li, C.; Hoover, A. N.; Webb, E.; Bose,
513 E. A.; Zeng, Y. Engineering, Characterizing Variability in Lignocellulosic Biomass: A Review. *ACS Sustainable*
514 *Chem. Eng.* **2020**, *8* (22), 8059-8085.
- 515 (7) Schreiber, M.; Vivekanandhan, S.; Mohanty, A. K.; Misra, M. A study on the electrospinning behaviour and
516 nanofibre morphology of anionically charged lignin. *Adv Mat Lett.* **2012**, *3*, 476.
- 517 (8) O'Connell, D. W.; Birkinshaw, C.; O' Dwyer, T. F. Heavy metal adsorbents prepared from the modification
518 of cellulose: A review. *Bioresour. Technol.* **2008**, *99* (15), 6709-6724.
- 519 (9) Alen, R.; Andersson, R.; Annergren, G.; Berg, C.-G.; Chirat, C.; van Dam, J.; Danielsson, M.; Engelfeldt,
520 A.; Engstrom, J.; Germgard, U., *Chemical pulping Part 1, fibre chemistry and Technology*; Paper Engineers'
521 Association/Paperi ja Puu Oy: Helsinki, 2011; Vol. 6.

- 522 (10) Mooney, C. A.; Mansfield, S. D.; Touhy, M. G.; Saddler, J. N. The effect of initial pore volume and lignin
523 content on the enzymatic hydrolysis of softwoods. *Bioresour. Technol.* **1998**, *64* (2), 113-119.
- 524 (11) Ben, H.; Chen, X.; Han, G.; Shao, Y.; Jiang, W.; Pu, Y.; Ragauskas, A. J. Characterization of whole biomasses
525 in pyridine based ionic liquid at low temperature by ³¹P NMR: an approach to quantitatively measure hydroxyl
526 groups in biomass as their original structures. *Front. Energy Res.* **2018**, *6*, 13.
- 527 (12) Balousek, P. J. The effects of ozone upon a lignin-related model compound containing a beta-aryl ether
528 linkage; Lawrence University: Appleton, 1979, pp. 3 - 4 (1979).
- 529 (13) Pouyet, F.; Chirat, C.; Potthast, A.; Lachenal, D. Formation of carbonyl groups on cellulose during ozone
530 treatment of pulp: Consequences for pulp bleaching. *Carbohydr. Polym.* **2014**, *109*, 85-91.
- 531 (14) Lemeune, S.; Jameel, H.; Chang, H. M.; Kadla, J., Effects of ozone and chlorine dioxide on the chemical
532 properties of cellulose fibers. *J APPL POLYM SCI* **2004**, *93* (3), 1219-1223.
- 533 (15) Abdolali, A.; Guo, W.; Ngo, H. H.; Chen, S.-S.; Nguyen, N. C.; Tung, K. L. Typical lignocellulosic wastes
534 and by-products for biosorption process in water and wastewater treatment: a critical review. *Bioresour. Technol.*
535 **2014**, *160*, 57-66.
- 536 (16) Gellerstedt, F.; Gatenholm, P. Surface properties of lignocellulosic fibers bearing carboxylic groups.
537 *Cellulose* **1999**, *6* (2), 103-121.
- 538 (17) Zhang 1, Y.; Sjögren, B.; Engstrand 2, P.; Htun, M. Determination of charged groups in mechanical pulp
539 fibres and their influence on pulp properties. *J. Wood Chem. Technol.* **1994**, *14* (1), 83-102.
- 540 (18) Belgacem, M.; Czeremuszkina, G.; Sapiuha, S.; Gandini, A. Surface by XPS characterization and inverse gas
541 of cellulose fibres chromatography. *Cellulose* **1995**, *2* (3), 145-157.
- 542 (19) Saha, P.; Chowdhury, S.; Gupta, S.; Kumar, I. Insight into adsorption equilibrium, kinetics and
543 thermodynamics of Malachite Green onto clayey soil of Indian origin. *Chem. Eng. J.* **2010**, *165* (3), 874-882.
- 544 (20) Wang, H.; Yuan, X.; Zeng, G.; Leng, L.; Peng, X.; Liao, K.; Peng, L.; Xiao, Z., Removal of malachite green
545 dye from wastewater by different organic acid-modified natural adsorbent: kinetics, equilibriums, mechanisms,
546 practical application, and disposal of dye-loaded adsorbent. *Environ. Sci. Pollut. Res.* **2014**, *21* (19), 11552-11564.
- 547 (21) Salima, A.; Benaouda, B.; Noureddine, B.; Duclaux, L. Application of *Ulva lactuca* and *Systocera stricta*
548 algae-based activated carbons to hazardous cationic dyes removal from industrial effluents. *Water Res.* **2013**, *47*
549 (10), 3375-3388.
- 550 (22) Neibi, M. C.; Mahjoub, B.; Seffen, M.; Kinetic and equilibrium studies of methylene blue biosorption by
551 *Posidonia oceanica* (L.) fibres. *J Hazard Mater.* **2007**, *139*(2), 280-285.
- 552 (23) Kumar, K.V.; Sivanesan, S.; Ramamurthi, V.; Adsorption of malachite green onto *Pithophora* sp., a fresh
553 water algae: equilibrium and kinetic modelling. *Process Biochem.* **2005**, *40*(8), 2865-2872.
- 554 (24) Ho, Y. S.; McKay, G. Pseudo-second order model for sorption processes. *Process Biochem.* **1999**, *34* (5),
555 451-465.
- 556 (25) Ho, Y. S. Second-Order Kinetic Model for the Sorption of Cadmium onto Tree Fern: A Comparison of Linear
557 and Non-Linear Methods. *Water Res.* **2006**, *40* (1), 119-125.
- 558 (26) Chowdhury, S.; Saha, P. Pseudo-Second-Order Kinetic Model for Biosorption of Methylene Blue onto
559 Tamarind Fruit Shell: Comparison of Linear and Nonlinear Methods. *Bioremediat. J.* **2010**, *14* (4), 196-207.
- 560 (27) Vadivelan, V.; Kumar, K. V. Equilibrium, kinetics, mechanism, and process design for the sorption of
561 methylene blue onto rice husk. *J. Colloid Interface Sci.* **2005**, *286* (1), 90-100.
- 562 (28) Aksu, Z.; Tezer, S. Equilibrium and kinetic modelling of biosorption of Remazol Black B by *Rhizopus*
563 *arrhizus* in a batch system: effect of temperature. *Process Biochem.* **2000**, *36* (5), 431-439.
- 564 (29) Namasivayam, C.; Kavitha, D. Removal of Congo Red from water by adsorption onto activated carbon
565 prepared from coir pith, an agricultural solid waste. *Dyes Pigm.* **2002**, *54* (1), 47-58.

- 566 (30) Dai, C.; Yang, L.; Xie, J.; Wang, T.-J. Physicochemical, S. A.; Aspects, E., Nutrient diffusion control of
567 fertilizer granules coated with a gradient hydrophobic film. *Colloids Surf., A* **2020**, *588*, 124361.
- 568 (31) Öner, M.; Doğan, Ö.; Öner, G. The influence of polyelectrolytes architecture on calcium sulfate dihydrate
569 growth retardation. *J. Cryst. Growth* **1998**, *186* (3), 427-437.
- 570 (32) Wågberg, L. Polyelectrolyte adsorption onto cellulose fibres - A review. *NORD PULP PAP RES J* **2000**, *15*
571 (5), 586-597.35.
- 572 (33) Lloyd J A, Horne C W. The determination of fibre charge and acidic groups of radiata pine pulps. *NORD*
573 *PULP PAP RES J*. **1993**, *08* (1), 048-052.
- 574 (34) Röhrling, J.; Potthast, A.; Rosenau, T.; Lange, T.; Borgards, A.; Sixta, H.; Kosma, P. A novel method for the
575 determination of carbonyl groups in celluloses by fluorescence labeling. 2. Validation and applications.
576 *Biomacromolecules* **2002**, *3* (5), 969-975.
- 577 (35) Liao, J.; He, S.; Mo, L.; Guo, S.; Luan, P.; Zhang, X.; Li, J. Mass-Production of High-Yield and High-
578 Strength Thermomechanical Pulp Fibers from Plant Residues Enabled by Ozone Pretreatment. *J. Cleaner Prod.*
579 **2021**, 126575.
- 580 (36) Freudenberg, K.; Neish, A. C. Constitution and biosynthesis of lignin. In Constitution and biosynthesis of
581 lignin; Springer: New York, 1968.
- 582 (37) Kocaefe, D.; Huang, X.; Kocaefe, Y.; Boluk, Y. Quantitative characterization of chemical degradation of
583 heat - treated wood surfaces during artificial weathering using XPS. *Surf. Interface Anal.* **2013**, *45* (2), 639-649.
- 584 (38) Ren, J.-L.; Sun, R.-C.; Peng, F. Carboxymethylation of hemicelluloses isolated from sugarcane bagasse.
585 *Polym. Degrad. Stab.* **2008**, *93* (4), 786-793.
- 586 (39) Laine, J.; Stenius, P.; Carlsson, G.; Ström, G. Surface characterization of unbleached kraft pulps by means
587 of ESCA. *Cellulose* **1994**, *1* (2), 145-160.
- 588
- 589

590 All figures and TOC graphic in this article is free domain

591 TOC graphic



592